

# The effect of the $\phi^4$ kink's internal mode during scattering on $\mathcal{PT}$ -symmetric defect

*D. Saadatmand*<sup>1)</sup>, *S. V. Dmitriev*<sup>+</sup>\*, *D. I. Borisov*<sup>×</sup>∇, *P. G. Kevrekidis*<sup>◦</sup>, *M. A. Fatykhov*<sup>∇</sup>, *K. Javidan*

*Department of Physics, Ferdowsi University of Mashhad, 91775-1436 Mashhad, Iran*

<sup>+</sup>*Institute for Metals Superplasticity Problems RAS, 450001 Ufa, Russia*

<sup>\*</sup>*National Research Tomsk State University, 634036 Tomsk, Russia*

<sup>×</sup>*Institute of Mathematics CC USC RAS, 450008 Ufa, Russia*

<sup>◦</sup>*Department of Mathematics and Statistics, University of Massachusetts, MA 01003 Amherst, USA*

<sup>∇</sup>*Bashkir State Pedagogical University, 450000 Ufa, Russia*

Submitted 29 December 2014

The effect of the  $\phi^4$  kink's internal mode (IM) during the scattering from a  $\mathcal{PT}$ -symmetric defect is investigated. It is demonstrated that if a  $\phi^4$  kink hits the defect from the gain side, a noticeable IM is excited, while for the kink coming from the opposite direction the mode excitation is much weaker. In the case when the kink initially carries IM, the IM amplitude is affected by the defect if the kink moves from the gain side and it is not affected when the kink moves in the opposite direction. A two degree of freedom collective variable model is shown to be capable of reproducing principal findings of the present work.

DOI: 10.7868/S0370274X15070140

**Introduction.** Over the last fifteen years, Bender and co-authors have explored broad classes of non-Hermitian Hamiltonians possessing real spectra under the parity-time ( $\mathcal{PT}$ ) symmetry condition, where parity-time means spatial reflection and time reversal [1, 2]. This mathematical discovery has generated an intense interest in the consideration of open physical systems with balanced gain and loss and such setting have been realized experimentally in optics [3–8], electronic circuits [9–11], and mechanical systems [12].

The Klein–Gordon field theory with a  $\mathcal{PT}$ -symmetric term, which describes a localized  $\mathcal{PT}$ -symmetric defect, has been recently introduced by one of the authors [13]. A collective coordinate method for nonconservative systems was developed in that work to describe the kink interaction with the defect, see also [14–16]. It was shown that standing kinks in such models are stable (unstable) if they are centered at the loss side (gain side) of the defect [15], while standing breathers may exist only if centered exactly at the interface between gain and loss regions [16].

The interaction of the moving kinks and breathers with the spatially localized  $\mathcal{PT}$ -symmetric perturbation was recently investigated in the realm of the sine-

Gordon (SG) equation [17]. Several new soliton-defect interaction scenarios were observed such as the kink passing/trapping depending on whether the kink comes from the gain or loss side of the impurity, merger of the kink-antikink pair into a breather, and splitting of the breather into a kink-antikink pair. The kink phase shift as a result of interaction with the impurity and the threshold kink velocity to pass through the lossy side of the defect were successfully calculated with the help of the collective variable approach [13, 17].

It is well-known that in the integrable SG model, the kink does not support vibrational internal modes (IM), while the kinks in the non-integrable  $\phi^4$  model do support such a mode [18]. It is for that reason that the kink-antikink interactions are far richer in the case of the  $\phi^4$  model [19–21]. When a kink hits an impurity in a conservative model, a part of its energy is trapped towards the excitation of the impurity mode [22, 23] and another fraction leads to the emission of radiation bursts [24]. It is of particular interest to investigate the role of the kink's IM in the case when the kink interacts with the  $\mathcal{PT}$ -symmetric impurity. This problem is addressed here for the  $\phi^4$  kinks.

The outline of the Letter is as follows. Firstly we introduce the spatially localized  $\mathcal{PT}$ -symmetric inhomogeneity into the  $\phi^4$  field and present the well-known  $\phi^4$

<sup>1)</sup>e-mail: saadatmand.d@gmail.com

kink solution and the kink's IM profile. Then a collective variable method is applied and analytically solved to reveal some features of the kink dynamics in this system. Next, we report on the numerical results for scattering of kinks on the  $\mathcal{PT}$ -symmetric defect. Finally, our conclusions and some future directions are presented.

**The model.** In this paper we study the modified  $\phi^4$  equation [13]

$$\phi_{tt} - \phi_{xx} - 2\phi(1 - \phi^2) = \epsilon\gamma(x)\phi_t, \quad (1)$$

where  $\phi(x, t)$  is the unknown scalar field, lower indices indicate partial derivatives with respect to the corresponding indices, and  $\gamma(x)$  is introduced as

$$\gamma(x) = \tanh(\beta x)\operatorname{sech}(\beta x), \quad (2)$$

which has the symmetry  $\gamma(-x) = -\gamma(x)$ . The latter identity means that the right hand side in (1) is a  $\mathcal{PT}$ -symmetric defect, i.e., it preserves its form under the change  $x \mapsto -x$  and  $t \mapsto -t$ . We also note that the same concerns the left hand side of equation (1). The physical meaning of equation (1) is that it describes an open system with gain and loss and the former balances the latter. The parameter  $\beta$  characterizes the defect inverse width.

As  $\gamma(x) \equiv 0$ , Eq. (1) is the non-integrable  $\phi^4$  equation with the following moving kink solution

$$\phi_K(x, t) = \pm \tanh\{\delta_k(x - x_0 - V_k t)\}, \quad (3)$$

where  $V_k$  is the kink velocity,  $x_0$  is the kink initial position and  $\delta_k = 1/\sqrt{1 - V_k^2}$ . Kink bearing IM can be approximately described as [20]

$$\Phi_K(x, t) = \phi_K(x, t) + A\xi(x, t)\sin(\omega t), \quad (4)$$

$$\begin{aligned} \xi(x, t) &= \sqrt{\frac{3}{2}} \tanh\{\delta_k(x - x_0 - V_k t)\} \times \\ &\times \operatorname{sech}\{\delta_k(x - x_0 - V_k t)\}. \end{aligned} \quad (5)$$

The IM has amplitude  $A$  and frequency  $\omega = \sqrt{3}$ . This mode has been discussed by many authors due to its critical role in the collision phenomenology of the  $\phi^4$  model [19–21]. In this Letter we show that the kink's IM noticeably affects the kink dynamics during the interaction with the  $\mathcal{PT}$ -symmetric defect.

**Collective variable method.** In [13] a two-degree of freedom collective variable model was offered and this model takes into account not only the kink's translational mode but also the kink's IM. The  $\phi^4$  kink is effectively described by the two degree of freedom particle of mass  $M = 4/3$ , which is the mass of the standing kink. The kink coordinate  $\mathcal{X}(t)$  (which in the unperturbed

case is given by  $x_0 + V_k t$  as a function of time  $t$ ) and the kink's internal shape mode  $A(t)$  are solutions to the equations

$$M\ddot{\mathcal{X}} = \epsilon \int_{-\infty}^{\infty} (\phi'_K + A\xi')[(\phi'_K + A\xi')\dot{\mathcal{X}} - \dot{A}\xi]\gamma(x)dx, \quad (6)$$

$$\ddot{A} = -\omega^2 A + \epsilon \int_{-\infty}^{\infty} \xi[-(\phi'_K + A\xi')\dot{\mathcal{X}} + \dot{A}\xi]\gamma(x)dx. \quad (7)$$

The first equation describes the kink translational mode and the latter characterizes the amplitude of the internal shape mode of the  $\phi^4$  kink. These equations yield the general form of the nonconservative forcing including the coupling between the modes. Once  $A$  is small enough, we can neglect the terms of order  $O(A)$  and it simplifies the above equations:

$$M\ddot{\mathcal{X}} = \epsilon\dot{\mathcal{X}} \int_{-\infty}^{\infty} [\phi'_K(x - \mathcal{X})]^2 \gamma(x)dx, \quad (8)$$

$$\ddot{A} = -\omega^2 A + \epsilon \int_{-\infty}^{\infty} [\xi(x - \mathcal{X})]^2 \gamma(x)dx. \quad (9)$$

Below we present the results of numerical solution for the two degree of freedom model (6) and (7).

**Numerical results.** To solve numerically Eq. (1) we introduce the mesh  $x = nh$ , where  $n = 0, \pm 1, \pm 2, \dots$  and  $h = 0.1$  is the selected spacing. The accuracy of the finite difference approximation used is  $O(h^4)$ . The resulting set of the ordinary differential equations is integrated numerically using the time step  $\tau = 0.005$  in the numerical scheme with the accuracy of  $O(\tau^4)$ . In the present study the simulations are carried out for fixed  $\beta = 1$  (the impurity width is approximately equal to the kink width).

To solve numerically the collective variable equations of motion Eqs. (6), (7), the temporal variable is discretized,  $t = j\tau$ , where  $j = 0, 1, 2, \dots$ . The second-order central differences are used to replace  $\ddot{\mathcal{X}} \sim (\mathcal{X}_{j-1} - 2\mathcal{X}_j + \mathcal{X}_{j+1})/\tau^2$ ,  $\dot{\mathcal{X}} \sim (\mathcal{X}_{j+1} - \mathcal{X}_{j-1})/2\tau$ , and similarly for  $\ddot{A}$  and  $\dot{A}$ . For the initial conditions to boost the kink with the initial velocity  $V_k$  and the initial IM amplitude  $A$ , we set  $\mathcal{X}(j = 0) = \mathcal{X}_0$ ,  $\mathcal{X}(j = 1) = \mathcal{X}_0 + V_k\tau$ ,  $A(j = 0) = A(j = 1) = A$ .

**Kinks bearing no initial IM.** Firstly we discuss the continuum model of Eq. (1). Fig. 1a and b) shows the kink kinetic energy as a function of time for the case when the kink, initially bearing no IM, interacts with the  $\mathcal{PT}$ -symmetric defect with amplitude  $\epsilon = 0.15$ . In panel a) the kink approaches the defect from the gain side and in panel b) from the loss side. The kink initial

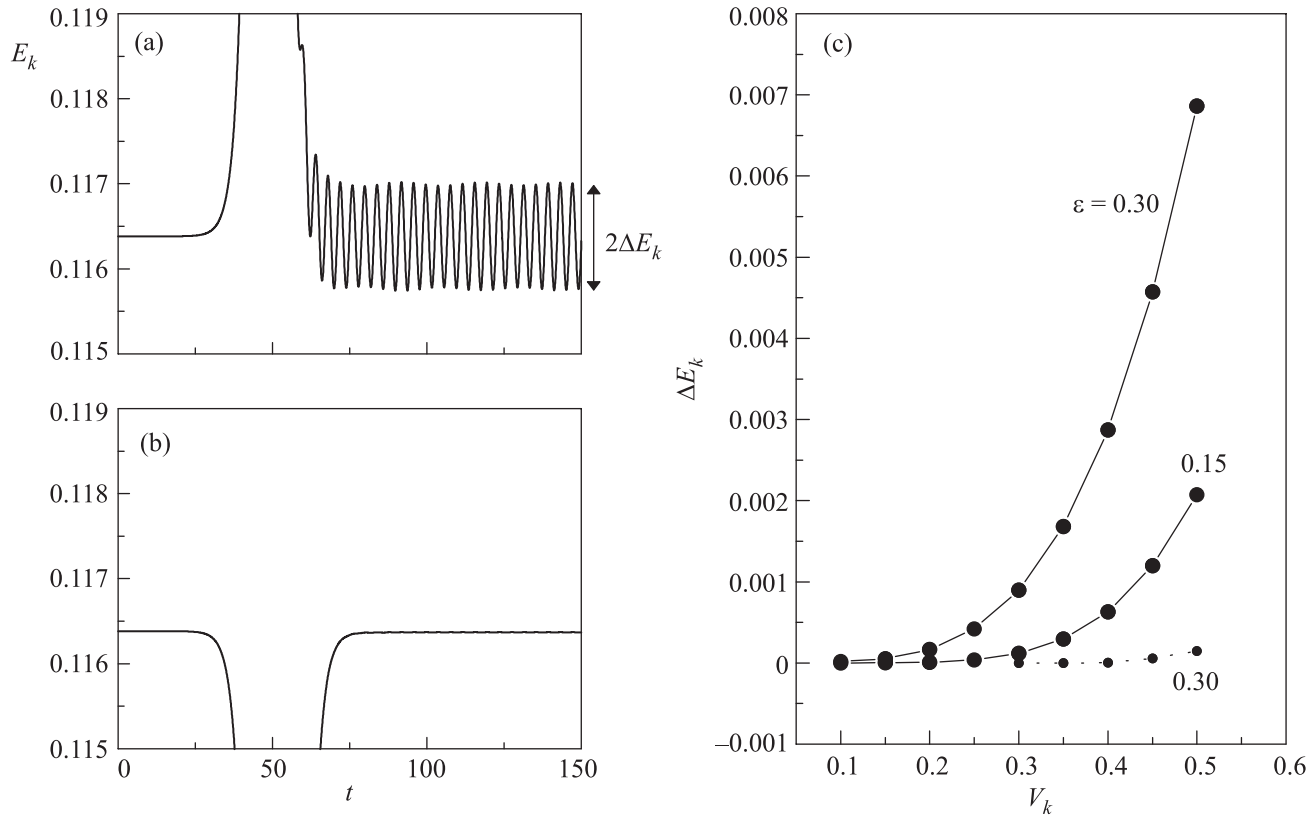


Fig. 1. Numerical results for the continuum model Eq. (1) showing the interaction of the kink initially bearing no IM with the  $\mathcal{PT}$ -symmetric defect. In panels a and b shown is the kink kinetic energy as a function of time for the defect amplitude  $\epsilon = 0.15$  and the kink initial velocity  $V_k = 0.4$ . The kink approaches the defect from the gain side (a) and from the loss side (b) of the defect. The figures reveal that in panel a kink's IM is excited after the interaction with the defect, while in panel b it is practically not excited. (c) – Amplitude of the kink kinetic energy after the interaction with the defect as a function of kink initial velocity for the case when kink hits the defect from the gain side (solid line) and loss side (dotted line) for  $\epsilon = 0.15$  and  $0.3$

velocity is  $V_k = 0.4$  in both cases. As a result of interaction with the defect, the kink in panel a is firstly accelerated and then decelerated, while in panel b it is first decelerated and then accelerated. In both cases the kink's translational velocity after passing through the defect is practically identical to the initial velocity. Note that the kink without the IM excited has a constant in time kinetic energy, while the kinetic energy of the kink with the excited IM oscillates near the constant value with frequency  $2\sqrt{3}$ , which is double the IM frequency. The intensity of the IM will be characterized by the amplitude of the kink kinetic energy oscillation caused by the IM,  $\Delta E_k = (E_{k,\max} - E_{k,\min})/2$ , where  $E_{k,\max}$  and  $E_{k,\min}$  are the maximum and minimum of the kink kinetic energy. In Fig. 1a the kink hits the defect from the gain side and a noticeable IM is excited as a result of the kink-defect interaction, while for the kink coming from the opposite direction (see Fig. 1b), the IM is much weaker and, in fact, cannot be seen in the scale of the figure. The ef-

fect of the kink's IM excitation as a result of the interaction with the defect becomes stronger for larger initial kink velocity  $V_k$  and larger defect amplitude  $\epsilon$ , as can be seen from Fig. 1c, where the kink kinetic energy oscillation amplitude  $\Delta E_k$  is shown as the function of  $V_k$  for  $\epsilon = 0.15$  and  $\epsilon = 0.3$ . Solid (dotted) lines show the results for the kink moving from the gain (loss) side. The log-log plot of the data shown in Fig. 1c reveals that for  $\epsilon = 0.3$ ,  $\Delta E_k \sim V_k^6$ . Since  $\Delta E_k \sim A^2$ , where  $A$  is the kink's IM amplitude, one has  $A \sim V_k^3$ . For  $V_k < 0.1$  the excitation of the kink's IM is very weak even for the kink moving from the gain side and even for the relatively large value of  $\epsilon$  such as  $\epsilon = 0.3$ .

The results obtained for the continuum system Eq. (1) and presented in Fig. 1 will be now compared to the results of the numerical solution of Eqs. (6), (7) for the two degree of freedom collective variable model, see Fig. 2. In panels a and b we plot the amplitude of the shape mode as a function of time. Here, the kink

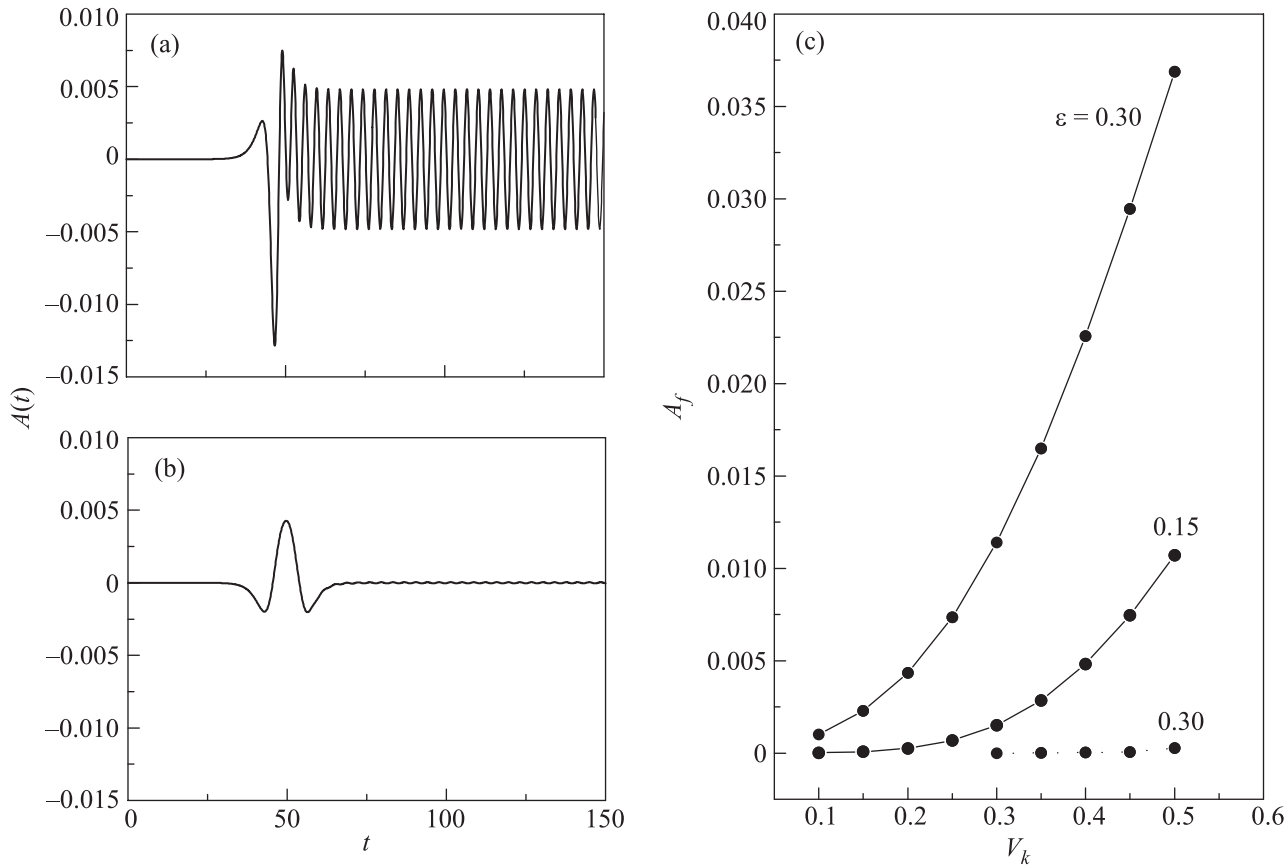


Fig. 2. Collective variable results for the model Eqs. (6), (7). (a, b) – The dynamics of the shape mode whose amplitude  $A(t)$  is shown for the case when the kink comes from gain side (a) and loss side (b). The perturbation amplitude is  $\epsilon = 0.15$  and the initial velocity of the kink is  $V_k = \pm 0.4$ . (c) – Amplitude of the shape mode after the interaction with the defect as a function of kink initial velocity for the case when the kink hits the defect from the gain side (solid line) and loss side (dotted line) for  $\epsilon = 0.15$  and  $0.3$

with initial velocity  $V_k = \pm 0.4$  hits the defect of amplitude  $\epsilon = 0.15$  from the gain side (Fig. 2a) and loss side (Fig. 2b). It can be seen that for the kink coming from the gain side a noticeable IM is excited after the interaction with the defect, whereas for the kink moving in the opposite direction the excited IM is much weaker and cannot be seen in the scale of the figure. This is in very good qualitative agreement with the results for continuum model. In Fig. 2c it is demonstrated that the kink's IM amplitude after the interaction with the defect increases with increase in  $V_k$  and  $\epsilon$ . The use of the log-log coordinates for Fig. 2c shows that  $A_f \sim V_k^3$ . Solid (dotted) lines show the results for the kink moving from the gain (loss) side. We could not provide a quantitative comparison of the models because it is possible only for  $V_k < 0.1$ , when the kink's IM amplitude in the continuum model does not depend on  $V_k$ . But, as it was mentioned above, the kink IM amplitude is extremely weak for  $V_k < 0.1$ .

**Kinks with initially excited IM.** Here, the scattering of a kink bearing an initial IM on a  $\mathcal{PT}$ -symmetric defect is considered. Again we start from the continuum model Eq. (1). We consider a kink with IM excited with the help of Eq. (4) using the IM amplitude  $A = 0.05$  and the kink initial velocity  $V_k = 0.3$ . The amplitude of the initial kink kinetic energy oscillation,  $\Delta E_k^i$ , is equal to 0.0033. This initial value is plotted in Fig. 3a with horizontal dotted lines. Now we calculate the value of  $\Delta E_k^f$  after the kink passes through the defect with the amplitude  $\epsilon = 0.15$  as a function of the kink initial position and present the results by solid line in Fig. 3a for the kink moving from the gain (thick line) and the loss (thin line) side of the defect. It is clear that the kink's IM is affected by the defect when it moves from the gain side because  $\Delta E_k^f$  differs from  $\Delta E_k^i$ , while in the opposite case the IM amplitude is practically not changed by the defect. The oscillation of  $\Delta E_k^f$  as a function of the kink initial position  $x_0$  has a period close to

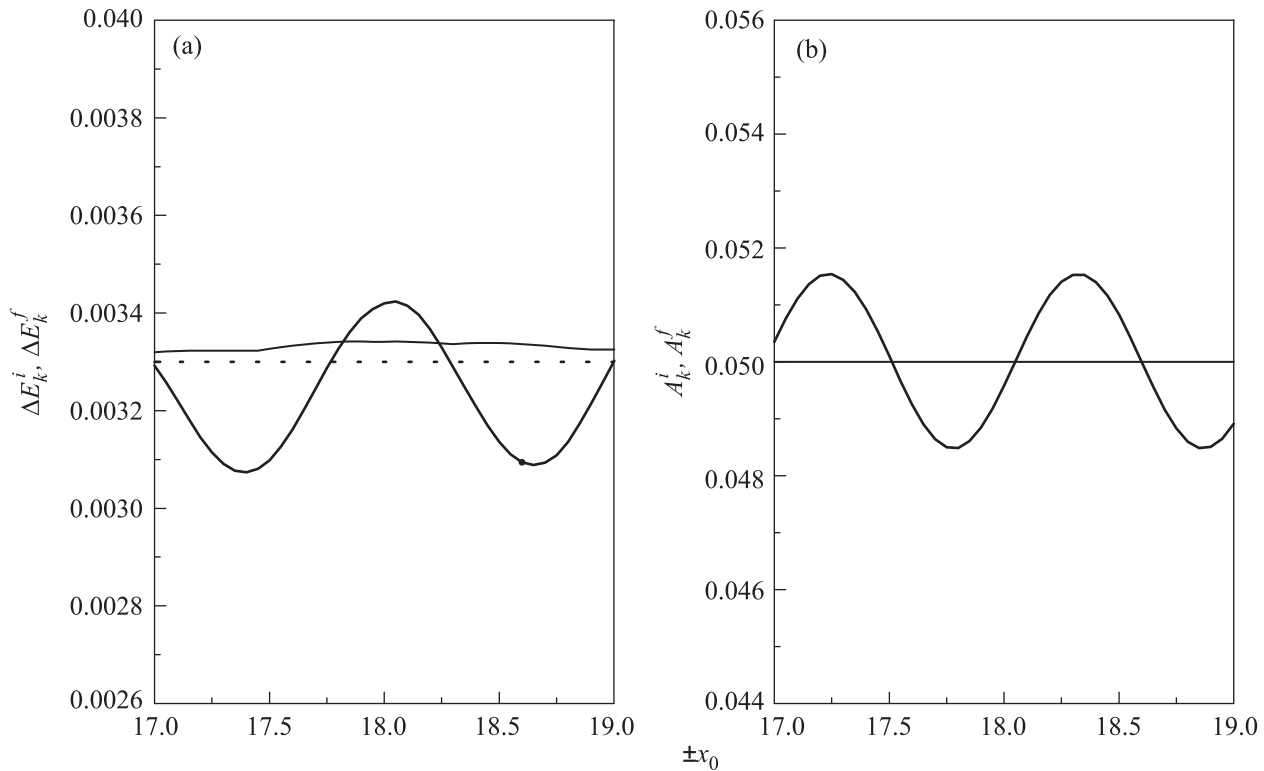


Fig. 3. (a) – Numerical results for the continuum model. Amplitude of the kink kinetic energy oscillation before ( $\Delta E_k^i$ , dotted line) and after ( $\Delta E_k^f$ , solid lines) the interaction with the  $\mathcal{PT}$ -symmetric defect as a function of kink initial position. Thick (thin) line shows the case when the kink moves from the gain (loss) side of the defect. (b) – Collective variable results for the model Eqs. (6), (7). The IM amplitude before ( $A_k^i$ , dotted line) and after ( $A_k^f$ , solid lines) the interaction with the defect as a function of the kink initial position. Thick line shows the case when the kink comes from the gain side and thin line (overlaps with the dotted line) shows the case when the kink comes from the loss side. Parameters used in panels a and b: the defect amplitude  $\epsilon = 0.15$  and the kink initial velocity  $V_k = 0.3$

$V_k(2\pi/\omega)$ , which is the distance the kink travels in one period of IM oscillation.

Similar results obtained in frame of the two degree of freedom collective variable model Eqs. (6), (7) are presented in Fig. 3b. The initial ( $A_k^i$ ) and final ( $A_k^f$ ) amplitudes of the kink's shape mode are shown as functions of the kink initial position by the dotted and solid lines, respectively. Thick (thin) solid lines show the results for the kink moving toward the defect with amplitude  $\epsilon = 0.15$  from the gain (loss) side. The kink initially has an IM of amplitude  $A = 0.05$  and the initial velocity of the kink is  $V_k = 0.3$ . In very good qualitative agreement with the results for continuum model, the collective variable model shows that the kink's IM is affected by the defect when it moves from the gain side and it does not when it moves in the opposite direction (the thin solid line overlaps with the dotted line).

**Conclusions.** The interaction of the  $\phi^4$  kinks with and without IM excitation with the  $\mathcal{PT}$ -symmetric defect was investigated numerically. It has been shown

that the kink's IM plays an important role during the scattering process. From our numerical results presented in Fig. 1 it follows that a noticeable IM is excited on the  $\phi^4$  kink after passing the defect from the gain side and the excitation of IM is much weaker for the kink moving in the opposite direction. The excitation of the kink's IM increases with increasing kink initial velocity  $V_k$  and the defect strength  $\epsilon$ , see Fig. 1c. These effects are well reproduced qualitatively by the two degree of freedom collective variable model Eqs. (6), (7), as shown in Fig. 2.

For the kink with an initially excited IM, the IM is affected by the defect when the kink hits the defect from the gain side, and the effect is stronger for faster kinks and larger defect strength (see Fig. 3a, thick solid line). In contrast, for the kink moving in the opposite direction, the initially excited IM is not affected by the defect (see Fig. 3a, thin solid line). Analogous results obtained with the use of the collective variable model are shown in Fig. 3b, and they are in very good qualitative agreement with the results for the continuum  $\phi^4$  model.

Quantitative comparison of the continuum and collective variable models is complicated because the kink's IM excitation is noticeable only for kink initial velocity  $V_k > 0.1$ , while the kink kinetic energy amplitude  $\Delta E_k$  can be related to the kink internal mode amplitude  $A$  only for  $V_k < 0.1$ , otherwise  $\Delta E_k$  depends not only on  $A$ , but also on  $V_k$ .

We conclude that the  $\mathcal{PT}$ -symmetric defects give new opportunities in the manipulation of the soliton dynamics and the presence of the internal modes can induce noticeable asymmetries of the solitary wave-defect interaction in terms of their excitation and overall time evolution.

D.S. thanks the hospitality of the Bashkir State Pedagogical University and acknowledges the financial support from the Institute for Metals Superplasticity Problems, Ufa, Russia. S.V.D. thanks financial support provided by the Russian Science Foundation, grant # 14-13-00982. D.I.B. thanks partially support provided by a grant of Russian Foundation for Basic Research, the grant of the President of Russian Federation for young scientists-doctors of science (project # MD-183.2014.1), and by the fellowship of Dynasty foundation for young Russian mathematicians. P.G.K. acknowledges support from the US National Science Foundation under grants # CMMI-1000337, DMS-1312856, from FP7-People under grant # IRSES-606096 from the Binational (US-Israel) Science Foundation through grant # 2010239, and from the US-AFOSR under grant # FA9550-12-10332.

- 
1. C. M. Bender and S. Boettcher, Phys. Rev. Lett. **80**, 5243 (1998).
  2. C. M. Bender, D. C. Brody, and H. F. Jones, Phys. Rev. Lett. **89**, 270401 (2002).
  3. C. E. Ruter, K. G. Markris, R. El-Ganainy, D. N. Christodoulides, M. Segev, and D. Kip, Nat. Phys. **6**, 192 (2010).
  4. B. Peng, S. K. Ozdemir, F. Lei, F. Monifi, M. Gianfreda, G. L. Long, S. Fan, F. Nori, C. M. Bender, and L. Yang, Nat. Phys. **10**, 394 (2014).
  5. B. Peng, S. K. Ozdemir, S. Rotter, H. Yilmaz, M. Liertzer, F. Monifi, C. M. Bender, F. Nori, and L. Yang, Science **346**, 328 (2014).
  6. A. A. Zyablovsky, A. P. Vinogradov, A. A. Pukhov, A. V. Dorofeenko, and A. A. Lisyansky, Phys. Usp. **57**(11), 1177 (2014).
  7. S. V. Dmitriev, A. A. Sukhorukov, and Yu. S. Kivshar, Opt. Lett. **35**(17), 2976 (2010).
  8. S. V. Suchkov, S. V. Dmitriev, B. A. Malomed, and Yu. S. Kivshar, Phys. Rev. A **85**, 033825 (2012).
  9. J. Schindler, A. Li, M. C. Zheng, F. M. Ellis, and T. Kottos, Phys. Rev. A **84**, 040101 (2011).
  10. J. Schindler, Z. Lin, J. M. Lee, H. Ramezani, F. M. Ellis, and T. Kottos, J. Phys. A: Math. Theor. **45**, 444029 (2012).
  11. N. Bender, S. Factor, J. D. Bodyfelt, H. Ramezani, D. N. Christodoulides, F. M. Ellis, and T. Kottos, Phys. Rev. Lett. **110**, 234101 (2013).
  12. C. M. Bender, B. Berntson, D. Parker, and E. Samuel, Am. J. Phys. **81**, 173 (2013).
  13. P. G. Kevrekidis, Phys. Rev. A **89**, 010102 (2014).
  14. A. Demirkaya, D. J. Frantzeskakis, P. G. Kevrekidis, A. Saxena, and A. Stefanov, Phys. Rev. E **88**, 023203 (2013).
  15. A. Demirkaya, M. Stanislavova, A. Stefanov, T. Kapitula, and P. G. Kevrekidis, Stud. Appl. Math. (in press); arXiv:1402.2942v1.
  16. N. Lu, J. Cuevas-Maraver, and P. G. Kevrekidis, J. Phys. A: Math. Theor. **47**, 455101 (2014).
  17. D. Saadatmand, S. V. Dmitriev, D. I. Borisov, and P. G. Kevrekidis, Phys. Rev. E **90**, 052902 (2014).
  18. T. Sugiyama, Prog. Theor. Phys. **61**, 1550 (1979).
  19. D. K. Campbell, J. S. Schonfeld, and C. A. Wingate, Phys. D **9**, 1 (1983).
  20. T. I. Belova and A. E. Kudryavtsev, Phys. Usp. **40**, 359 (1997).
  21. R. H. Goodman and R. Haberman, SIAM J. Appl. Dyn. Sys. **4**, 1195 (2005).
  22. Z. Fei, Yu. S. Kivshar, and L. Vazquez, Phys. Rev. A **45**, 6019 (1992).
  23. Yu. S. Kivshar, Z. Fei, and L. Vazquez, Phys. Rev. Lett. **67**, 1177 (1991).
  24. B. A. Malomed, Phys. D **15**, 385 (1985).